Noncoherent Sequence Detection Receiver for Bluetooth Systems

Lutz Lampe, Member, IEEE, Robert Schober, Member, IEEE, and Mani Jain

Abstract—The design of power efficient receivers for Bluetooth systems is a challenging task due to stringent complexity constraints. In this paper, we tackle this problem and present a receiver design consisting of a single filter and a subsequent noncoherent sequence detector. This receiver outperforms the conventional discriminator detector by more than 4 dB for typical Bluetooth channels. Thereby, the proposed noncoherent sequence detection (NSD) algorithm is both favorably low complex as it operates on a two-state trellis and highly robust against channel phase variations caused by low-cost local oscillators. The particular filter design accomplishes effective out-of-band interference suppression. Different from previous work on sequence detector receivers published in the literature, we take possible variations of the Bluetooth modulation parameters into account, and we also devise efficient methods for combined NSD and forward error correction decoding. Hence, the presented receiver design is an attractive solution for practical Bluetooth devices.

Index Terms—Adaptive receivers, Bluetooth systems, continuous phase modulation (CPM), Gaussian frequency-shift keying (GFSK), noncoherent sequence detection (NSD).

I. INTRODUCTION

B LUETOOTH [1] is an increasingly popular and widely deployed standard for wireless personal area networks (WPANs). The Bluetooth physical layer employs Gaussian frequency-shift keying (GFSK), which is a particular form of continuous phase modulation (CPM) [2]. GFSK provides a favorable tradeoff between power and bandwidth efficiency, and allows for low-complexity transmitter and receiver implementations. In fact, in practice a simple discriminator detector [3] is often used to recover the GFSK modulated data.

Though structurally and computationally simple, discriminator detectors are highly suboptimum as far as power efficiency is concerned. It is well known that sequence detectors are significantly more efficient [2]. However, realizing sequence detection (SD) for Bluetooth systems is a quite formidable task. The modulation index h for GFSK modulation is allowed to vary in a relatively wide interval, which leads to a varying trellis structure for SD with a possibly tremendous number of states. The optimal receiver filters for a sufficient statistic after sampling also depend on h and moreover, they might not accomplish sufficient out-of-band interference suppression. Furthermore, Blue-

Manuscript received March 25, 2004; revised November 17, 2004. This work was supported in part by the Natural Sciences and Engineering Research Council (NSERC) of Canada under Grant STPGP 257684 and Grant RGPIN 283152-04. This paper was presented in part at the IEEE Global Telecommunications Conference (GLOBECOM), Dallas, TX, 2004.

The authors are with the Department of Electrical and Computer Engineering, University of British Columbia, Vancouver, BC V6T 1Z4, Canada (e-mail: Lampe@ece.ubc.ca).

Digital Object Identifier 10.1109/JSAC.2005.853791

tooth's frequency hopping and the allowed local oscillator (LO) dynamics make it difficult to establish a phase reference, which is required for coherent SD.

There are several approaches to coherent SD for Bluetooth available in the literature, e.g., [4]–[6]. All of them accomplish low-complexity reduced-state SD. However, the respective designs are restricted to particular nominal values of h and, since coherent in nature, assume perfect channel phase estimation at the receiver. Therefore, their practical applicability is limited.

In this paper, we propose and study a noncoherent SD (NSD) receiver for Bluetooth systems, which in contrast to previous proposals does not require explicit channel phase estimation. We present a low-complexity implementation with only one receiver filter and NSD on a two-state trellis, which accomplishes significant performance gains of more than 4 dB over the discriminator-based detector. We further extend beyond previous work in that we: 1) consider the entire range of possible modulation indexes h; 2) provide an adaptive solution to account for varying h; 3) incorporate a frequency-offset compensator into NSD to cope with the unusually large LO frequency deviations envisaged in Bluetooth systems; and 4) devise improved decoding methods for the forward error correction (FEC) schemes employed in Bluetooth. Simulation and analytical results verify that the presented NSD receiver operates close to the theoretical limits and is an attractive and robust solution for power-efficient Bluetooth devices.

This paper is organized as follows. In Section II, we introduce the Bluetooth transmission model. The NSD receiver is presented in Section III, and the performance of this receiver is studied for Bluetooth specific scenarios in Section IV. Finally, Section V concludes the paper.

II. BLUETOOTH TRANSMISSION MODEL

For the application of SD to GFSK, we first introduce the adopted GFSK signal description in Section II-A. Then, Section II-B briefly reviews the FEC schemes employed in Bluetooth, and the Bluetooth specific channel model is described in Section II-C. Finally, Section II-D refers to the benchmark detectors considered in this paper.

A. GFSK Modulation

The passband GFSK signal has the form [2]

$$s_{\mathsf{RF}}(t) = \frac{\sqrt{2E_s}}{T} \cos\left(2\pi f_c t + 2\pi h \sum_{i=0}^{\infty} a[i]q(t-iT)\right) \tag{1}$$

where E_s denotes the signal energy per modulation interval T, f_c is the carrier frequency, h is the modulation index, and $a[i] \in$

 $\{\pm 1\}$ represent the binary data. The normalized phase pulse $q(t)=\int_{-\infty}^t g(\tau)\mathrm{d}\tau$ is obtained from the frequency impulse

$$g(t) = \frac{1}{2T} \left(\mathbf{Q} \left(\gamma \cdot B \left(t - \frac{T}{2} \right) \right) - \mathbf{Q} \left(\gamma \cdot B \left(t + \frac{T}{2} \right) \right) \right) \tag{2}$$

with constant $\gamma = 2\pi/\sqrt{\log(2)}$ and Q(x) is the Gaussian Q-function. In the Bluetooth standard [1], the 3-dB-band-width-time product is specified as BT = 0.5 with $T = 10^{-6}$ s, whereas the modulation index h can vary between 0.28 and 0.35.

Since $q(LT) \simeq 1/2$ is true for L=2, we can well approximate GFSK as partial response CPM with a truncated frequency pulse of duration LT and L=2 [4]. Furthermore, to make the considered GFSK scheme amenable to sequence detection, the modulation index is appropriately quantized, such that h is expressed as rational number h=k/p with relatively prime integers k and p (see Section IV for numerical examples). Using the transformation frequency $f_0=f_c-(h/2T)$, the equivalent complex baseband (ECB) GFSK transmitter can be decomposed into a 2p-state trellis and a memoryless mapper with 4p time-limited, constant envelope signal elements $\rho_{m(\boldsymbol{b}[i])}(t)$, $\rho_{m(\boldsymbol{b}[i])}(t)=0$ for t<0 and t>T, $1\leq m(\boldsymbol{b}[i])\leq 4p$, cf. [8] and [9]. The address vector

$$\mathbf{b}[i] = [b[i], b[i-1], \psi[i]] \tag{3}$$

is determined by the current and the previous modified binary data symbols

$$b[i] = \frac{a[i]+1}{2} \in \{0,1\} \tag{4}$$

and by the p-ary phase state

$$\psi[i] = \left(k \sum_{j=0}^{i-2} b[j]\right) \bmod p. \tag{5}$$

Applying this decomposition, the ECB transmit signal can be written as

$$s(t) = \sum_{i=0}^{\infty} \rho_{m(\boldsymbol{b}[i])}(t - iT). \tag{6}$$

B. Forward Error Correction (FEC)

The two FEC schemes employed in Bluetooth are a rate 1/3 repetition code and a rate 2/3 expurgated (15,10) Hamming code [1], [10]. In the asynchronous data link, the repetition code protects the header of data packets. The Hamming code is applied to the payload of data medium (DM) rate packet types, but no FEC coding is used for the payload of data high (DH) rate packet types. For synchronous speech or data transmission, the payload is uncoded, repetition coded, or Hamming coded depending on the packet type.

 1 Larger values of L, e.g., L=3 [7], would increase receiver complexity but provide almost no performance gain.

C. Channel Model

The typical application environment for Bluetooth renders the transmission channel frequency nonselective with a static fading gain for the duration of one packet, e.g., [11], [12]. The first-order statistics of the fading gain is typically modeled by a Ricean distribution with Ricean factor K including the additive white Gaussian noise (AWGN) channel ($K=\infty$) and Rayleigh-fading (K=0) as special cases, e.g., [13] and [14]. Since the radio-frequency requirements in the Bluetooth standard are fairly relaxed, we further need to account for frequency offsets and oscillator phase noise. Also, following the Bluetooth standard, we include co-channel and adjacent channel interference by other Bluetooth devices into our considerations. The ECB received signal is, therefore, modeled as

$$r(t) = g e^{j\phi(t)} s(t) + i(t) + n(t), \qquad 0 \le t \le T_p \qquad (7)$$

where the fading gain $g \in \mathbb{R}$ is constant over the packet length T_p and independent from packet-to-packet, $\phi(t)$ is the time-varying phase, n(t) is AWGN, and i(t) represent the collective interference. Denoting the frequency offset by Δf , the phase is appropriately described by the relation

$$\phi(t+\tau) = \phi(t) + 2\pi\Delta f \tau + \Delta\phi(t,\tau) \tag{8}$$

where for given t and τ $\Delta\phi(t+i\tau,\tau)$, $i\in \mathbf{Z}$, is a white Gaussian random process with variance $\sigma_{\Delta}^2(\tau)=(2\pi f_c)^2c\tau$ and c is a constant depending on the employed oscillator, e.g., [15]. As robust and low-cost solutions are desired for Bluetooth applications, we assume that $\phi(t)$ is not attempted to be estimated at the receiver, i.e., noncoherent detection with unknown $\phi(t)$ is performed.

D. Benchmark Receivers

As already mentioned in Section I, the limiter-discriminator with subsequent integrate and dump filtering (LDI) [3] is a popular low-cost and robust noncoherent receiver for Bluetooth communication systems, e.g., [13]. Therefore, the LDI receiver is considered as simple-to-implement, practical benchmark scheme for the receiver structure proposed in the next section.

For application in Bluetooth systems Scholand *et al.* have recently proposed a so-called max-log-maximum-likelihood LDI (MLM-LDI) detector [7], which consists of a zero-crossing detector followed by digital integrate and dump filtering and a postprocessor. This postprocessor involves a forward-backward (FB) algorithm on a four-state trellis, whose complexity is higher than that of the two-state Viterbi algorithm for NSD devised in this paper. However, since the MLM-LDI detector achieves significant performance gains over the conventional LDI receiver, the bit-error rate (BER) results presented in [7, Fig. 1] will also be used for a performance comparison in Section IV.

Furthermore, we measure the proposed NSD receiver against the theoretical performance limit, which is coherent maximumlikelihood sequence detection (MLSD) assuming optimum filtering and perfect channel estimation [2].

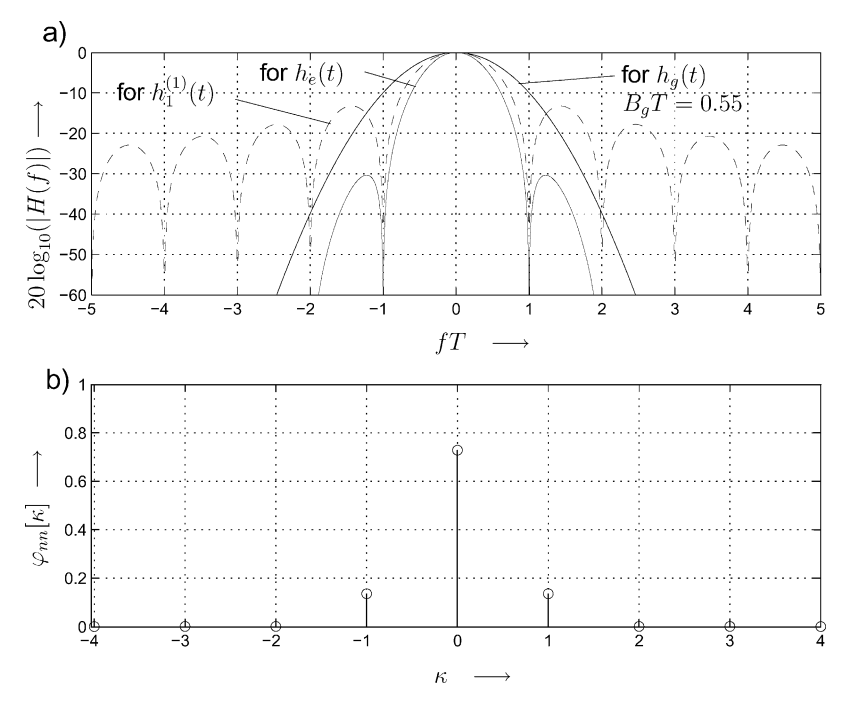


Fig. 1. (a) Magnitude frequency responses for different receiver filters. (b) Noise autocorrelation function $\varphi_{nn}[\kappa]$ after filter $h_e(t)$ and sampling.

III. NONCOHERENT SEQUENCE DETECTION RECEIVER

The decomposition approach [8], [9] for GFSK suggests a receiver consisting of a bank of D=4p matched filters $^2h_D^{(d)}(t)=\rho_d^*(-t), \ 1\leq d\leq D,$ and a subsequent sequence detector with 2p states. The complexity of such a receiver quickly becomes prohibitive, e.g., p=100 for h=0.29. To solve this problem, a suitable filter design and reduced state NSD algorithm are derived in Sections III-A and III-B, respectively. Furthermore, to account for varying modulation index h, an adaptive NSD algorithm is presented in Section III-C. Finally, an appropriate combination of NSD with FEC decoding is devised in Section III-D. We also provide the BER MLSD lower bound for the AWGN channel, which proves to be a valuable tool for the design and performance analysis of NSD.

A. Filter Design

The large number of filters can be tremendously reduced with only negligible performance loss by using time-limited complex exponential functions³

$$h_D^{(d)}(t) = \frac{1}{T} \mathrm{e}^{\mathrm{j} 2\pi f_d t}, \, f_d = \frac{\sigma}{2} (2d - 1 - D), \, -\frac{T}{2} \leq t \leq \frac{T}{2} \ \, (9)$$

where the frequency spacing σ is to be optimized. This approach was successfully advocated in [16] and [17]. In particular, the use of only one filter, i.e., D=1, yields already excellent performance results for the considered GFSK modulation (see results in Section IV) and, thus, we will focus on this choice in the following.

Although well suited to represent the GFSK signal space, the filters in (9) can accomplish only limited adjacent channel in-

terference suppression. Therefore, as a pragmatic solution, we apply an additional Gaussian prefilter

$$h_g(t) = \sqrt{\frac{2\pi}{\log(2)}} B_g e^{-\frac{2\pi^2}{\log(2)}(B_g t)^2}$$
 (10)

with 3-dB bandwidth B_g , which is typically used in combination with the LDI receiver, e.g., [3] and [13]. For D=1, the effective receiver filter $h_e(t)=h_g(t)*h_1^{(1)}(t)$ is obtained as $(\gamma=2\pi/\sqrt{\log(2)})$

$$h_e(t) = \frac{1}{T} \left(Q \left(\gamma \cdot B_g \left(t - \frac{T}{2} \right) \right) - Q \left(\gamma \cdot B_g \left(t + \frac{T}{2} \right) \right) \right). \tag{11}$$

To illustrate the filter characteristics for this case, Fig. 1(a) shows the magnitude frequency response of the filters $h_1^{(1)}(t)$ (9), $h_g(t)$ (10), and $h_e(t)$ (11), respectively, for a typical value of $B_gT=0.55$ [13]. The combined filter $h_e(t)$ has virtually the same passband characteristics as $h_1^{(1)}(t)$, but the stopband characteristics are significantly improved. On the other hand, since $h_e(t)$ is not time-limited and $h_e(t)*h_e^*(-t)$ is not a Nyquist pulse, intersymbol interference (ISI) and colored additive noise will occur after sampling. Fortunately, these effects are minor as can be seen from the rapidly decaying noise autocorrelation function depicted in Fig. 1(b) (again $B_gT=0.55$ is assumed). For this reason and for the sake of a simple implementation, we neglect ISI and noise coloring in the following NSD design (but of course not in the performance study in Section IV).

B. Noncoherent Sequence Detection

From filtering and sampling we obtain the discrete-time received signal vector $\mathbf{r}[i] = [r^{(1)}[i] \dots r^{(D)}[i]]$, with scalar $\mathbf{r}[i] = r^{(1)}[i]$ for the most interesting case of D = 1. For the derivation of NSD, we assume the noise and interference con-

 $^{^2\}mathrm{In}$ this paper, .* and .^H refer to complex conjugation and Hermitian transposition, respectively.

 $^{^3 \}rm{For}$ convenience, we specify the receiver low-pass filters with respect to the carrier frequency $f_c.$

tained in r[i] to be white Gaussian and/or perfectly suppressed and, for the moment, a constant phase $\phi(t) = \phi_0$. Under these assumptions, the maximum-likelihood (ML) noncoherent sequence detector for a block of N_T data symbols maximizes the metric (Re $\{\cdot\}$: real part of a complex number) [18]

$$\Lambda[N_T] = \operatorname{Re} \left\{ \sum_{i=1}^{N_T} \boldsymbol{r}[i] \boldsymbol{\rho}_{m(\tilde{\boldsymbol{b}}[i])}^H q_{\text{ref}}^*[i-1] \right\}.$$
 (12)

In (12), $\rho_{m(\boldsymbol{b}[i])}$ is the vector of the D coordinates representing the signal element $\rho_{m(\boldsymbol{b}[i])}(t)$ with respect to the D receive filters [16], [17], $\tilde{\boldsymbol{b}}[i]$ contains the hypothetical data, and $q_{\text{ref}}[i-1]$ can be interpreted as an estimate of $\mathrm{e}^{\mathrm{j}\phi_0}$.

1) Branch Metric: In case of coherent detection, i.e., ϕ_0 is perfectly known, we have $q_{\rm ref}[i] = {\rm e}^{{\rm j}\phi_0}$ and the standard Viterbi algorithm with branch metric

$$\lambda[i] = \operatorname{Re}\left\{ \mathbf{r}[i] \mathbf{\rho}_{m(\tilde{\mathbf{b}}[i])}^{H} q_{\text{ref}}^{*}[i-1] \right\}$$
 (13)

can be applied to maximize (12). Such an approach, with a different receiver filter, is advocated in [4] and [5].

In order to realize NSD without the need for explicit phase estimation and to account for the time variance of $\phi(t)$, the use of the Viterbi algorithm with the recursively updated phase reference

$$q_{\mathsf{ref}}[i] = \alpha q_{\mathsf{ref}}[i-1] + (1-\alpha) r[i] \rho_{m(\tilde{\boldsymbol{b}}[i])}^{H}$$
 (14)

in (13) was proposed [17]. The parameter α , $0 \le \alpha < 1$, acts as forgetting factor and its choice trades performance for constant phase offset and robustness against phase variations [17].

NSD with (14) is highly power efficient and fairly insensitive to phase noise and frequency offset. However, the frequency offset Δf allowed in Bluetooth systems is in the order of ± 100 kHz, i.e., the normalized offset ΔfT can be as large as ± 0.1 . To cope with such tremendous frequency deviations it is mandatory to incorporate the effect of Δf into the definition of the phase reference. Therefore, we propose here the modified reference symbol

$$q_{\text{ref}}[i] = \left(\alpha q_{\text{ref}}[i-1] + (1-\alpha)\boldsymbol{r}[i]\boldsymbol{\rho}_{m(\tilde{\boldsymbol{b}}[i])}^{H}\right) e^{\mathrm{j}2\pi\widehat{\Delta f}[i-1]}$$

$$\tag{15}$$

with the frequency offset estimate

$$e^{j2\pi\widehat{\Delta f}[i]} = \frac{p_{\text{ref}}[i]}{|p_{\text{ref}}[i]|}$$
 (16)

obtained by the adaptive estimator

$$p_{\text{ref}}[i] = \beta p_{\text{ref}}[i-1] + (1-\beta)\boldsymbol{r}[i]\boldsymbol{\rho}_{m(\tilde{\boldsymbol{b}}[i])}^{H}(\boldsymbol{\rho}_{m(\tilde{\boldsymbol{b}}[i-1])}\boldsymbol{r}^{H}[i-1]).$$
(17)

Similarly, to the role of α for $q_{\text{ref}}[i]$, the adjustment of the parameter β , $0 \le \beta < 1$, enables to balance the performance for constant frequency offset and the ability to track oscillator drifts. By using the reference phase (15) in the branch metric (13), NSD is still robust against random phase noise and residual frequency offset $(\Delta f - \widehat{\Delta f})$, but explicitly accounts for the most prominent and systematic contributor to phase variations in Bluetooth systems (see discussion in Section IV).

We would like to point out that the chosen approach is similar to frequency estimation for NSD and linear modulation ad-

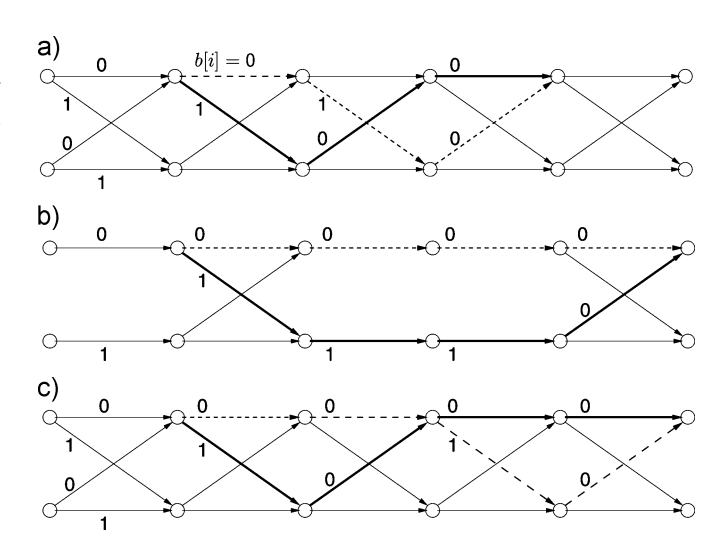


Fig. 2. Two-state trellis for NSD of GFSK. Dashed and bold lines indicate most-likely error events. (a) Uncoded transmission or conventional decoding. (b) Joint NSD and decoding of repetition code. (c) Hamming code with modified decoding.

vocated by Colavolpe and Raheli in [19]. Moreover, at typically required signal-to-noise power ratios (SNRs) the estimator (17) resembles Kay's frequency estimator [20], which was also found advantageous in [19]. Both (15) and (17) are different from [19] and [20], respectively, in that recursive update equations are formulated, which 1) involve less arithmetic operations than the window processing methods of [19] and [20] and 2) are especially well suited for per-state tracking in the (reduced-state) trellis of NSD. It is also worth noting that the devised frequency offset estimation for NSD corresponds to the use of DC offset cancellation methods for the LDI receiver.

2) State Reduction: Regardless whether a perfect phase reference is assumed or whether NSD with (15) is applied, full state sequence detection with 2p states is not feasible for Bluetooth with modulation indexes $0.28 \le h \le 0.35$. However, reduction to only two states is readily accomplished by employing per-survivor processing (PSP) [21]. In particular, the proposed NSD uses tentative decisions on the phase state according to the survivor path terminating in the current state. In doing so, NSD is performed on the two-state trellis depicted in Fig. 2(a) regardless of the actual modulation index h = k/p.

At this point, it is worth mentioning that explicit phase estimation, which is a formidable task anyway, becomes practically impossible for reduced-state sequence detection and large p. Due to the small distance between stable phase points, frequent phase slips are very likely to occur. Therefore, an implicit phase estimation as with (15) is mandatory.

C. Adaptive NSD

For the preceding derivation of the NSD receiver, the modulation index h was assumed to be known, i.e., estimation of h is required. Alternatively, the sequence detector could operate with an assumed nominal value \hat{h} of h, regardless of its actual value. Since h is allowed to vary in the interval $0.28 \le h \le 0.35$, considerable performance degradations might result for large deviations from the nominal value (see results in Section IV).

An appealing compromise between the two approaches, and as such between complexity and power efficiency, is to perform NSD for a small number of different hypotheses $\tilde{h} \in \mathcal{H}$ and after an estimation period of N_e symbols to adaptively choose the hypothesis yielding the maximum metric (12)

$$(\hat{b}[1], \dots, \hat{b}[N_e], \hat{h}) = \underset{\tilde{b}[1] \dots \tilde{b}[N_e], \tilde{h} \in \mathcal{H}}{\operatorname{arg max}} \left\{ \operatorname{Re} \left\{ \sum_{i=1}^{N_e} \boldsymbol{r}[i] \boldsymbol{\rho}_{m(\tilde{\boldsymbol{b}}[i])}^H q_{\text{ref}}^*[i-1] \right\} | \tilde{h} \right\}. \quad (18)$$

In (18), ${\bf r}[i]$ and ${\bf \rho}_{m(\tilde{{\bf b}}[i])}$ depend on \tilde{h} via the demodulation frequency $f_0=f_c-(\tilde{h}/2T)$ and the assumed signal elements ${\bf \rho}_{m(\tilde{{\bf b}}[i])}(t)$, respectively, and $q^*_{\rm ref}[i]$ depends on \tilde{h} through ${\bf r}[i]$ and ${\bf \rho}_{m(\tilde{{\bf b}}[i])}$. After the estimation period, the best estimate \hat{h} is used for detecting the entire transmitted sequence. This adaptive NSD can be regarded as approximate ML joint detection and estimation with quantization of the unknown parameter. For a reasonably small number of tested hypotheses and short estimation periods, e.g., $|\mathcal{H}|=2$ and $N_e=10\dots50$, the complexity increase due to adaptation is almost negligible.

It is interesting to note that because of the demodulation of the passband received signal with $f_0 = f_c - (\hat{h}/2T)$, a modulation index mismatch results in an effective frequency offset $\Delta f = (\hat{h} - h)/2T$. Since the proposed NSD with phase reference (15) compensates for frequency offsets, it also implicitly alleviates this detrimental effect of a modulation index mismatch. Of course, the mismatch with respect to the assumed signal space cannot be corrected.

D. Decoding

In a conventional setup, the FEC decoder uses hard-decision estimates of the binary symbols b[i] (or equivalently, a[i], see Section II-A) to retrieve the encoded data. Furthermore, the error correction capability of the repetition or Hamming code is utilized to correct single errors only. However, this direct approach to FEC decoding is ill-suited for NSD. An examination of the GFSK trellis reveals that the most likely error events are $[b[i], b[i+1], b[i+2]] \leftrightarrow [\overline{b}[i], \overline{b}[i+1], b[i+2]]$ for $b[i+1] = \overline{b}[i]$, i.e., strict double errors are caused $(\overline{b}[i]$ denotes the complement of b[i]). For example, the error event $[010] \leftrightarrow [100]$ is indicated in Fig. 2(a). Thus, when using single-error correction hard-decision decoding subsequent to NSD neither repetition nor Hamming coding improve the error rate over uncoded transmission. For the sake of brevity, we refer to this decoding scheme as conventional decoding in the following.

1) MLSD Bound: Before we devise enhanced decoding strategies, it is helpful to have an estimate for the achievable BER. As coding and decoding are performed independently for each Bluetooth packet, it is appropriate to consider the MLSD bound for the AWGN channel, which is given by [2, Ch. 3]

$$BER \ge C \cdot Q\left(\sqrt{\frac{d_{\min}^2(h)}{R_c} \frac{E_s}{\mathcal{N}_0}}\right). \tag{19}$$

In (19), $d_{\min}(h)$ is the minimum normalized Euclidean distance between two possible sequences of binary symbols b[i] during

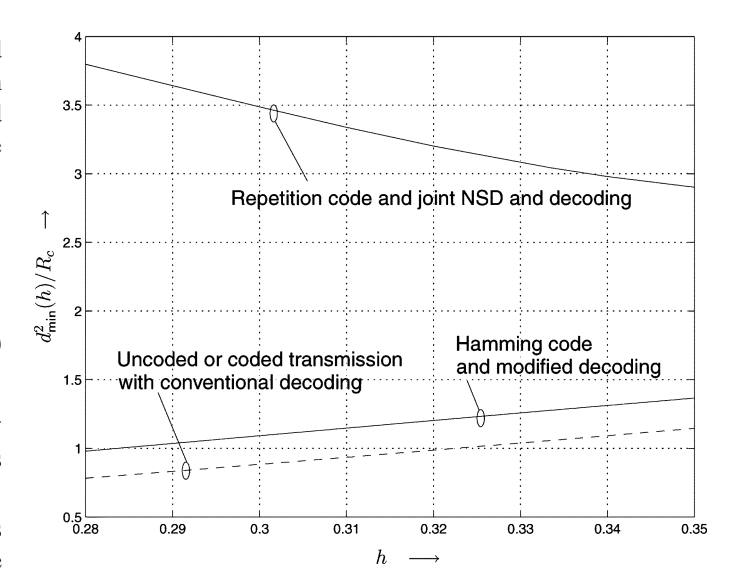


Fig. 3. Normalized minimum Euclidean distance $d_{\min}^2(h)/R_c$ as function of modulation index h for different coding and decoding schemes.

SD, R_c denotes the code rate, and \mathcal{N}_0 is the two-sided power spectral density of the ECB noise. The positive constant C has a minor influence on BER as it accounts for the number of bit errors per error event and their dependence on the transmitted data.

We would like to point out that (19) is valid for coherent SD. Therefore, it is also a bound for NSD, which 1) is tight for reliable phase references (15) and 2) allows for a valuable quantitative comparison of different coding and decoding schemes in combination with NSD (see discussion in Section IV). Also, note that we consider the energy per coded symbol E_s instead of the usually used energy per information bit E_b to enable a comparison of the different coding schemes for fixed received power.

From (19), we infer that the detection efficiency is compactly represented by the normalized minimum Euclidean distance [2, Ch. 3]. For, respectively, uncoded transmission and coded transmission with conventional decoding, this minimum distance corresponds to the error event illustrated in Fig. 2(a). This error event is identical for the two-state trellis and the full state trellis, i.e., the minimum distance is not decreased due to state reduction. The resulting parameter $d_{\min}^2(h)/R_c$ is shown in Fig. 3 as function of the modulation index h (dashed line, e.g., [2, Ch. 3] for calculation of $d_{\min}^2(h)$). For example, for h=0.32, we have $d_{\min}^2(h=0.32)/R_c=0.99$.

2) Repetition Code: The structural simplicity of the repetition code allows to readily include the code constraints into NSD yielding a joint GFSK and FEC decoder. The underlying trellis is depicted in Fig. 2(b). The most likely error event corresponds now to sequences $[b[i], b[i+1], b[i+2], b[i+3]] \leftrightarrow [\overline{b}[i], \overline{b}[i+1], \overline{b}[i+2], b[i+3]]$, where due to encoding b[i] = b[i+1] = b[i+2] is enforced. The parameter $d_{\min}^2(h)/R_c$ for this error event is plotted in Fig. 3 (top curve). As can be seen, the minimum Euclidean distance is tremendously increased by including the code constraints into NSD. For example, considering h = 0.32, the distance $d_{\min}^2(h = 0.32)/R_c = 3.20$ is obtained, which corresponds to an improvement by about 5 dB in power efficiency over conventional decoding. Interestingly, now the min-

TABLE I
REPRESENTATION OF MODULATION INDEX FOR NSD

h	0.28	0.29	0.30	0.31	0.32	$0.3\bar{3}$	0.34	0.35
k/p	7/25	29/100	3/10	31/100	8/25	1/3	17/50	7/20

imum distance is monotonic decreasing in h, which can be attributed to an accumulated phase difference of $3 \cdot (2\pi h)$ for the two admissible sequences [0,0,0] and [1,1,1].

As can easily be seen from a comparison of the trellises in Fig. 2(a) and (b), the number of required branch-metric calculations per symbol interval is reduced if joint decoding is performed. Thus, the gains in power efficiency come even with a reduction in computationally complexity compared to conventional decoding.

3) Hamming Code: As implicitly done for the repetition code, joint decoding for the case of the Hamming code should conveniently be based on its trellis representation, e.g., [22]. However, the cyclic Hamming code specified in the Bluetooth standard [1] leads to a joint time-varying trellis with up to 32 states. Decoding on this trellis requires on average the calculation of almost 34 branch metrics per symbol interval as opposed to only four in the conventional decoding case. Therefore, in light of the stringent complexity constraints imposed on Bluetooth systems, joint decoding is not advisable in this case.

Fortunately, it is feasible to improve hard-decision decoding subsequent to NSD. The fact that Bluetooth employs the expurgated (15,10) and not the original (15,11) Hamming code renders the correction of up to 31 error patterns possible. We can, thus, apply the standard syndrome decoder for the cyclic Hamming code, e.g., [10, Ch. 5.2], but extend the syndrome detection unit to also account for the double-error events identified at the beginning of Section III-D and illustrated in Fig. 2(a). In this way, the most-likely error events of NSD can be corrected if the data is protected by the Hamming code.

From the distance properties of GFSK signals, we find that the next likely error event is of the type $[b[i], b[i+1]] \leftrightarrow [\bar{b}[i], b[i+1]]$ for b[i+1] = b[i], which apparently incurs a single erroneous decision. However, this error event also implicates a phase slip, i.e., the phase state of the survivor path differs from the correct state by $2\pi h$, which due to PSP affects further decisions. In fact, a careful study shows that another error event compensating for the phase slip occurs with almost unit probability. Such a sequence of two error events cannot be corrected and, thus, the single-error event determines the minimum distance effective for the modified Hamming decoder. Fig. 2(c) shows a typical example for two such error events.

The increase in the minimum distance due to modified Hamming decoding is illustrated in Fig. 3. The gains are consistently in the order of 1 dB in power efficiency, which is moderate but comes at no increase in decoding complexity.

It is clear from the preceding discussion that the found minimum distance event for modified Hamming decoding is not present if full-state NSD is performed. The same is true for repetition coding and joint decoding, except for h=1/3. However, since full-state NSD is not a viable alternative, we refer to (19) with $d_{\min}^2(h)$ from Fig. 3 as MLSD bound also in the coded case.

IV. PERFORMANCE STUDY

In this section, the performance of the proposed NSD receiver is evaluated for different Bluetooth system specific scenarios. We first consider uncoded transmission in Section IV-A and concentrate on the efficiency and robustness of filter design, NSD, and adaptive NSD, as introduced in Sections III-A–III-C, respectively. Next, the performance of the devised FEC decoding schemes for NSD are discussed in Section IV-B. As for each Bluetooth packet a constant channel gain is observed (see Section II-C), we consider the AWGN channel as appropriate scenario to evaluate the proposed receiver design. Finally, the performance of NSD in fading channels is highlighted in Section IV-C.

In the following, we quantize the modulation index h in the relevant range in steps of 0.01, except for the obviously convenient choice $h=0.3\overline{3}=1/3$, which gives the rational numbers shown in Table I. In all cases, we apply NSD in the reduced two-state trellis (see Fig. 2). If not stated otherwise, the single (D=1) receive filter $h_e(t)$ (11) is applied. When comparisons with the LDI receiver are made, we assume an implementation of the LDI receiver and a Gaussian prefilter with 3-dB bandwidth $B_qT=0.55$, as described in [13].

A. Uncoded Transmission

In this section, we consider Bluetooth without FEC coding, which 1) is relevant for uncoded Bluetooth packet types and 2) allows to highlight the properties of NSD. As figure of merit, we consider the receiver SNR E_s/N_0 required to achieve a raw bit-error rate (BER) of BER = 10^{-3} , as required by the Bluetooth standard [1].

1) Noncoherent Sequence Detection: In order to study and separate the effects of the NSD design, Fig. 4 shows the required SNR for BER = 10^{-3} as a function of the modulation index h for, respectively, 1) the MLSD lower bound (19); 2) the NSD receiver with D=3 filters $h_3^{(d)}(t)$ and $\sigma T=0.5$ according to (9) and phase reference (14); 3) the NSD receiver with D=1 filter $h_e(t)$ and phase reference (14); and 4) the NSD receiver with D=1 filter $h_e(t)$ and phase reference (15). For a comparison, the required SNRs for the LDI receiver and for the MLM-LDI detector [7] (SNR points taken from [7, Fig. 1]) are also included. Constant channel phase $\phi(t) \equiv \phi_0$ and no interference are assumed.

First, let us consider NSD with phase reference (14). Comparing the two SNR curves for $\alpha=0.9$, we observe that a single receive filter, i.e., D=1, is practically sufficient to approximate the GFSK signal space. Moreover, the application of the Gaussian prefilter for interference suppression does not lead to any noticeable performance degradations. It can also be seen that the MLSD bound, which implies the use of 4p matched filters and idealized coherent detection, is well approached in the entire interval $0.28 \le h \le 0.35$. This result nicely confirms our approach of filtering and subsequence reduced-state NSD.

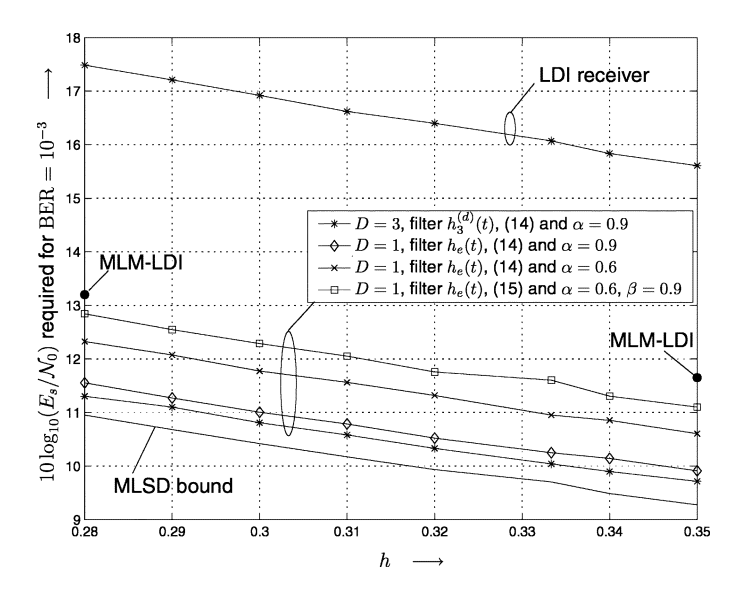


Fig. 4. Performance of proposed NSD as function of h. AWGN channel with time-invariant channel phase.

As expected, BER degrades with decreasing α due to less averaging in the implicit phase estimation, cf. (14).

NSD with phase reference (15) is somewhat less efficient than NSD with (14) for the considered case of constant channel phase. This is due to phase noise inherently caused by the embedded frequency estimator (16), (17). However, for the chosen parameters $\alpha=0.6$ and $\beta=0.9$, which offer high robustness against oscillator instabilities (see Section IV-A2), gains of more than 4 dB over the benchmark LDI receiver are consistently obtained. Furthermore, also the more complex MLM-LDI receiver with four-state FB trellis decoding is outperformed by the NSD receiver. In contrast to the proposed direct SD approach, the BER performance of the MLM-LDI receiver cannot approach the MLSD bound, but is limited by the suboptimum receiver front-end.

In the following, NSD with the single filter $h_e(t)$ is exclusively considered.

2) NSD in the Presence of Channel Phase Variations: The above results confirmed the high efficiency of the NSD receiver in an idealized scenario. However, the necessity for NSD derives from the relaxed Bluetooth specifications with respect to radio frequency stability. Fig. 5 illustrates the performance of the proposed NSD in unknown frequency offset Δf and possibly additional phase jitter with variance $\sigma_{\Delta}^2(T)$. Exemplarily, h=1/3 is chosen. For a comparison, the performance curves for the LDI receiver and the MLSD bound are also shown.

We can observe that NSD with phase reference (14) provides some robustness against moderate frequency offset, but cannot cope with offsets as large as 100 kHz, i.e., $\Delta fT=0.1$, which have to be tolerated according to the Bluetooth specification. In fact, with $\alpha=0.2$ the losses in power efficiency due to oscillator instabilities are very similar to those experienced by the LDI receiver. On the other hand, NSD with phase reference (15) successfully compensates even high-frequency offsets. The BER performance is virtually independent of Δf in the entire range $0 \leq \Delta fT \leq 0.1$ and close to the MLSD bound, which presumes perfect synchronization. Moreover, additional phase jitter results

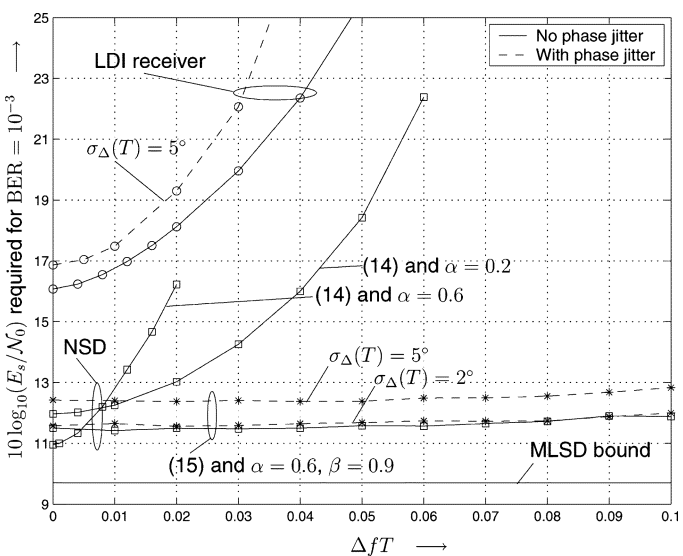


Fig. 5. Performance of proposed NSD in the presence of frequency offset Δf and phase jitter with variance $\sigma_{\Delta}^2(T)$. h=1/3 and single receiver filter $h_e(t)$.

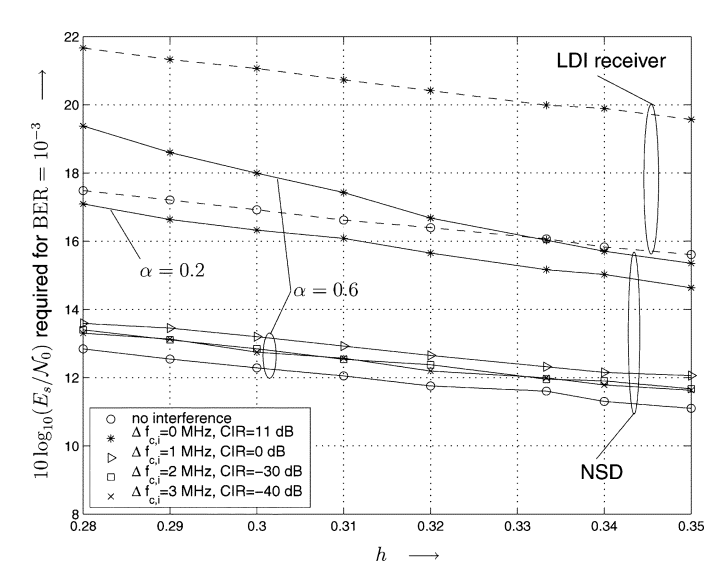


Fig. 6. Performance of proposed NSD in the presence of interference. Single receiver filter $h_e(t)$ and NSD with phase reference (15) and $\beta=0.9$.

in a fairly moderate loss in power efficiency. Thereby we note that, respectively, $\sigma_{\Delta}=2^{\circ}$ and 5° correspond to a single-sideband phase noise of -115 and -107 dBc/Hz at 3 MHz offset [15], whereas measured phase noise of well-designed integrated oscillators for Bluetooth is below -120 dBc/Hz at 3 MHz offset, e.g., [23]. We can, thus, conclude that the application of NSD with (15) is very well suited for Bluetooth systems. Therefore, we focus on this configuration in the following.

3) NSD in the Presence of Interference: Next, we consider transmission with Bluetooth interference. The carrier-to-interference power ratio (CIR) and the carrier frequency difference $\Delta f_{c,i}$ are chosen as specified in the Bluetooth standard [1]. Fig. 6 shows the performance results in terms of the required SNR over the modulation index h. As reference curves, the BERs for LDI without and with co-channel interference (CCI) are included.

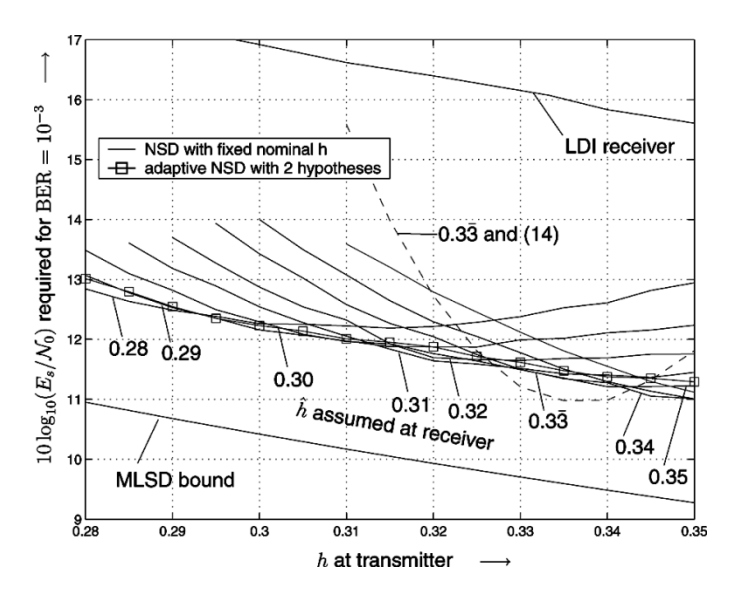


Fig. 7. Performance of NSD and adaptive NSD for unknown modulation index h. Single receiver filter $h_e(t)$ and NSD with phase reference (15), $\alpha=0.6$, and $\beta=0.9$.

The results in Fig. 6 verify the effective adjacent channel interference (ACI) suppression due to the applied receiver filter. The loss due to ACI is about 1 dB and, since it mainly depends on the filter characteristics, it is fairly independent of α (15) and β (17).⁴ In the case of CCI, the experienced performance losses are similar to those for the LDI receiver. Here, smaller values of α are found advantageous. This behavior can be explained by the fact that the decision metric becomes more mismatched with increasing α , as a less time-variant channel is assumed.

4) Adaptive NSD: If NSD assumes a modulation index \hat{h} deviating from the actual h at the transmitter, power efficiency deteriorates, as illustrated in Fig. 7 for the parameters $\alpha=0.6$ and $\beta=0.9$. For large deviations of more than, e.g., $|\hat{h}-h|\gtrsim 0.04$, we observe rapidly growing performance degradations which make adaptive NSD desirable.

Fig. 7 therefore shows the results for adaptive NSD with only two hypotheses and an estimation length of $N_e=30$ symbols (see Section III-C). As can be seen, adaptive NSD achieves practically optimum performance in the entire range of interest. Hence, uncertainties due to unknown and time-varying modulation index h can be fully compensated with only very little increase in complexity. In fact, we observed (not shown) that similar results as presented in Fig. 7 can also be obtained with even shorter estimation periods of, e.g., 10...15 symbols. It is also worth pointing out that adaptive NSD exhibits the same robustness against channel phase dynamics as NSD assuming perfectly known modulation index h (see results in Fig. 5).

Finally, Fig. 7 also includes the performance curve for NSD with (14) for $\hat{h}=1/3$. As it was anticipated in Section III-C, the phase reference symbol (14) is considerably more sensitive to a modulation index mismatch and is, thus, less suited for application to Bluetooth.

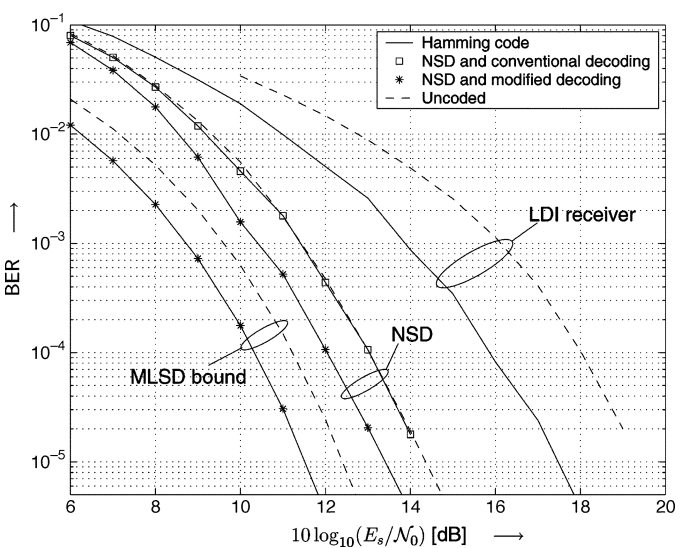


Fig. 8. Comparison of Hamming coded and uncoded transmission. Conventional and improved FEC decoding. Modulation index h=1/3, NSD with phase reference (15), $\alpha=0.6$, and $\beta=0.9$.

B. Coded Transmission

In this section, we evaluate the performance when an FEC scheme is applied. To this end, we utilize the MLSD bound (19) with the normalized minimum distances plotted in Fig. 3 together with simulation results. For the simulation results, we assume a transmission scenario as in Fig. 4 for uncoded transmission, i.e., static channel phase and no interference.

First, we consider the Hamming code, which is applied to the payload data and voice packets. Fig. 8 presents the BER for NSD with subsequent conventional and modified Hamming decoding as introduced in Section III-D3. For a comparison, the respective MLSD bounds and the BERs achieved with the LDI receiver are also shown. The modulation index is fixed to h=1/3. In accordance with the results from the trellis inspection in Section III-D3, conventional decoding does not yield any improvement over uncoded transmission if NSD is applied. On the other hand, as well predicted by the MLSD bound and the minimum distance analysis, modified decoding enables a gain of about 1 dB in power efficiency. This is about 1 dB short of the coding gain seen for the LDI receiver, but NSD offers still a considerable advantage of about 4 dB.

The results for the repetition code, which is mainly used to protect the header of Bluetooth data packets, are presented in Fig. 9. The BER achieved with joint decoding described in Section III-D2 is plotted as function of h for $10\log_{10}(E_s/\mathcal{N}_0)=6$ dB and 10 dB, respectively. The lower SNR value allows simulation of the BER and we observe that the MLSD bound quite accurately predicts the actual performance of NSD. Hence, the tremendous gains expected from the minimum distance analysis are indeed realized by joint decoding. Considering the MLSD bound for $10\log_{10}(E_s/\mathcal{N}_0)=10$ dB, we can conclude that the probability of a corrupted packet header is negligibly low for SNRs required to reliably transmit payload.

⁵In case of LDI detection, single errors, which can be corrected by conventional Hamming decoding, are more likely than for NSD.

 $^{^4}$ It is worth mentioning that ACI significantly deteriorates the performance for the considered LDI receiver with a relatively large 3 dB bandwidth of the prefilter (see results, e.g., [13]). In fact, reducing the prefilter bandwidth improves ACI suppression, while still providing robustness against frequency offset Δf , e.g., [24].

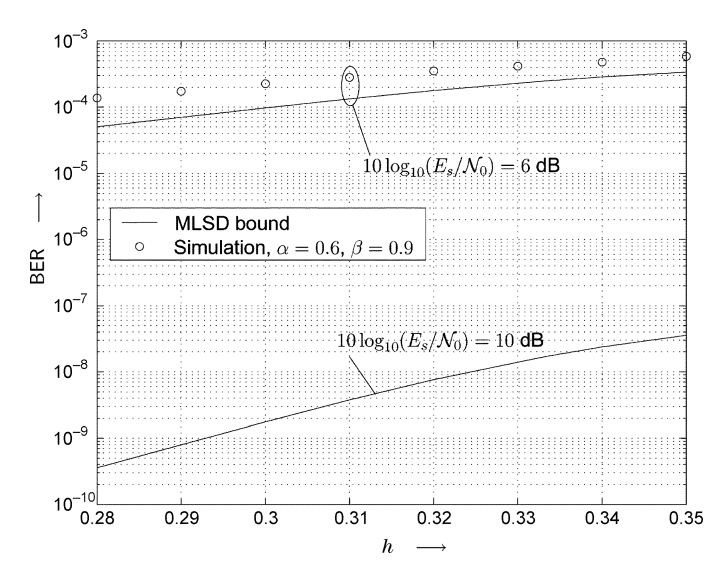


Fig. 9. Transmission with the repetition code and joint NSD and FEC decoding.

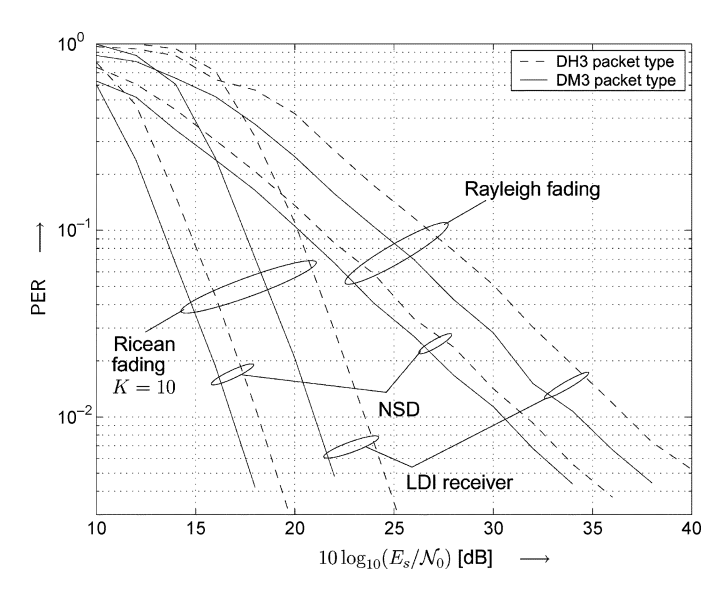


Fig. 10. PER for DM3 and DH3 packet types [1]. Modulation index h=1/3, NSD with phase reference (15), $\alpha=0.6$, and $\beta=0.9$.

C. Packet Transmission Over Fading Channels

Finally, we study the performance of the proposed NSD receiver for fading channels. With individual packets experiencing static fading the packet error rate (PER) is the appropriate performance parameter. Exemplarily, we consider Bluetooth DM and DH packet types with an occupation of three time slots, i.e., DM3 and DH3, respectively. The payload of DM3 packets is protected with the Hamming code, the payload of DH3 packets is uncoded. The packet length is 1500 payload symbols plus header and access code. According to the results in Section IV-B, the packet header, which is coded with the repetition code, can be safely assumed error free after decoding if the payload is correctly recovered.

Fig. 10 depicts the simulated PER over $10 \log_{10}(E_s/\mathcal{N}_0)$ for the relevant examples of Rayleigh fading and Ricean fading with Rice factor K=10, and both NSD and LDI receiver are considered. The comparison of the respective performance curves

reveals: 1) that the gains of the proposed NSD receiver derived from BER results for the AWGN channel are well reflected in an improved PER for fading channels and 2) that, as it was observed in Section IV-B, the Hamming code provides a coding gain of about 1 and 2 dB in combination with the NSD and the LDI receiver, respectively. Hence, we can conclude that the enhanced power efficiency of the NSD receiver directly translates into an increased data throughput and/or an improved coverage for Bluetooth systems.

V. CONCLUSION

The design of power efficient receivers for Bluetooth systems is a challenging task due to the stringent complexity constraints and the quite relaxed specifications of the modulation parameters in the Bluetooth standard. In this paper, we tackled this problem and presented an enhanced receiver design consisting of a single filter and a subsequent noncoherent sequence detector. The suggested filter front-end accomplishes a favorable tradeoff between effective signal-space representation and strong adjacent channel interference suppression. In contrast to previous approaches, the proposed NSD requires no channel phase estimation, which, on the one hand, makes efficient state reduction regardless of the GFSK modulation index h possible and, on the other hand, leads to high robustness against channel phase variations due to instable local oscillators. The adaptive NSD solution allows for fast adaptation of NSD to the actually used h and fully inherits the robustness and performance features of the nonadaptive algorithm assuming static or known h. Furthermore, we devised improved methods for combined NSD and FEC decoding. Comparisons with the LDI receiver for uncoded and coded transmission over typical Bluetooth channels showed significant performance gains of more than 4 dB in power efficiency. We, therefore, believe that the presented receiver design is an attractive solution for low-complexity yet power-efficient Bluetooth devices.

REFERENCES

- Bluetooth Special Interest Group, Specifications of the Bluetooth System, Version 1.2, Nov. 2003.
- [2] J. B. Anderson, T. Aulin, and C.-E. Sundberg, *Digital Phase Modulation*. New York: Plenum, 1986.
- [3] M. K. Simon and C. C. Wang, "Differential versus limiter-discriminator detection of narrowband FM," *IEEE Trans. Commun.*, vol. COM–31, no. 11, pp. 1227–1234, Nov. 1983.
- [4] A. Soltanian and R. E. Van Dyck, "Performance of the Bluetooth system in fading dispersive channels and interference," in *Proc. IEEE Global Telecommun. Conf.*, Nov. 2001, pp. 3499–3503.
- [5] W. Jia, A. Nallanathan, and H. K. Garg, "Performance of a Bluetooth system in multipath fading channels with interference," in *Proc. Int.* Workshop Mobile Wireless Commun. Netw., Sep. 2002, pp. 579–582.
- [6] R. Schiphorst, F. W. Hoeksema, and C. G. Slump, "A (simplified) Bluetooth maximum a posteriori probability (MAP) receiver," in Proc. IEEE Workshop Signal. Process. Adv. Wireless Commun., Rome, Italy, Jun. 2003, pp. 160–164.
- [7] T. Scholand, A. Waadt, and P. Jung, "Max-log-ML symbol estimation postprocessor for intermediate frequency LDI detectors," *Electron. Lett.*, vol. 40, no. 5, pp. 183–184, Feb. 2004.
- [8] J. B. Huber and W. Liu, "Convolutional codes for CPM using the memory of the modulation process," in *Proc. IEEE Global Telecommun. Conf.*, Tokyo, 1987, pp. 43.1.1–43.1.5.
- [9] B. E. Rimoldi, "A decomposition approach to CPM," *IEEE Trans. Inf. Theory*, vol. 34, no. 2, pp. 260–270, Mar. 1988.

- [10] S. B. Wicker, Error Control Systems for Digital Communication and Storage. Upper Saddle River, NJ: Prentice-Hall, 1995.
- [11] G. J. M. Janssen, P. A. Stigter, and R. Prasad, "Wideband indoor channel measurements and BER analysis of frequency selective multipath channels at 2.4, 4.75, and 11.5 GHz," *IEEE Trans. Commun.*, vol. 44, no. 10, pp. 1272–1288, Oct. 1996.
- [12] H.-J. Zepernick and T. A. Wysocki, "Multipath channel parameters for the indoor radio at 2.4 GHz ISM band," in *Proc. IEEE Veh. Technol. Conf.*, May 1999, pp. 190–193.
- [13] A. Soltanian and R. E. Van Dyck, "Physical layer performance for coexistence of Bluetooth and IEEE 802.11b," presented at the Symp. Wireless Pers. Commun., Blacksburg, VA, Jun. 2001.
- [14] A. Conti, D. Dardari, G. Pasolini, and O. Andrisano, "Bluetooth and IEEE 802.11b coexistence: Analytical performance evaluation in fading channels," *IEEE J. Sel. Areas Commun.*, vol. 21, no. 2, pp. 259–269, Feb. 2003.
- [15] A. Demir, A. Mehrotra, and J. Roychowdhury, "Phase noise in oscillators: A unifying theory and numerical methods for characterization," *IEEE Trans. Circuits Syst.*, vol. 47, no. 5, pp. 655–674, May 2000.
- [16] J. B. Huber and W. Liu, "An alternative approach to reduced-complexity CPM-receivers," *IEEE J. Sel. Areas Commun.*, vol. 7, no. 9, pp. 1437–1449, Dec. 1989.
- [17] L. Lampe, R. Schober, G. Enzner, and J. Huber, "Coded continuous phase modulation with low-complexity noncoherent reception," *IEEE Trans. Commun.*, vol. 50, no. 4, pp. 517–520, Apr. 2002.
- [18] G. Colavolpe and R. Raheli, "Noncoherent sequence detection of continuous phase modulations," *IEEE Trans. Commun.*, vol. 47, no. 9, pp. 1303–1307, Sep. 1999.
- [19] —, "Detection of linear modulations in the presence of strong phase and frequency instabilities," *IEEE Trans. Commun.*, vol. 50, no. 10, pp. 1617–1626, Oct. 2002.
- [20] S. Kay, "A fast and accurate single frequency estimator," *IEEE Trans. Acoust., Speech, Signal Process.*, vol. 37, no. 12, pp. 1987–1990, Dec. 1989
- [21] R. Raheli, A. Polydoros, and C.-K. Tzou, "Per-survivor processing: A general approach to MLSE in uncertain environments," *IEEE Trans. Commun.*, vol. 43, no. 2/3/4, pp. 354–364, Feb./Apr. 1995.
- [22] J. Wolf, "Efficient maximum-likelihood decoding of linear block codes using a trellis," *IEEE Trans. Inf. Theory*, vol. 24, no. 1, pp. 76–80, Jan. 1978.
- [23] D. M. W. Leenaerts, C. S. Vaucher, H. J. Bergveld, M. Thompson, and K. Moore, "A 15-mW fully integrated I/Q synthesizer for Bluetooth in 0.18-\(\mu\)mCMOS," IEEE J. Solid-State Circuits, vol. 38, no. 7, pp. 1155–1162, Aug. 2003.
- [24] M. Shimizu, N. Aoki, K. Shirakawa, Y. Tozawa, N. Okubo, and Y. Daido, "New method of analyzing BER performance of GFSK with postdetection filtering," *IEEE Trans. Commun.*, vol. 45, no. 4, pp. 429–436, Apr. 1997.



Lutz Lampe (S'98–M'02) received the Diplom (Univ.) and the Ph.D. degrees in electrical engineering from the University of Erlangen, Erlangen, Germany, in 1998 and 2002, respectively.

He is currently an Assistant Professor in the Department of Electrical and Computer Engineering, University of British Columbia, Vancouver, BC, Canada. His main research interests lie in the areas of communications and information theory applied to wireless and power-line transmission. This includes coding and decoding techniques for power- and

bandwidth-efficient transmission, space-time coded modulation, detection and estimation techniques, multicarrier modulation, and multiuser detection.

Dr. Lampe received the Best Student Paper Award at the European Wireless Conference 2000 and at the International Zurich Seminar 2002. In 2003, he received the Dissertation Award from the of the German Society of Information Techniques (ITG). He is an Associate Editor for the IEEE TRANSACTIONS ON VEHICULAR TECHNOLOGY, and serves as Vice Chair of the IEEE Communications Society Technical Subcommittee on power-line communications.



Robert Schober (S'98–M'01) was born in Neuendettelsau, Germany, in 1971. He received the Diplom (Univ.) and the Ph.D. degrees in electrical engineering from the University of Erlangen–Nurnberg, Erlangen, Germany, in 1997 and 2000, respectively.

From May 2001 to April 2002, he was a Postdoctoral Fellow at the University of Toronto, Toronto, ON, Canada, sponsored by the German Academic Exchange Service (DAAD). Since May 2002, he has been an Assistant Professor and Canada Research Chair (Tier II) in Wireless Communication at the

University of British Columbia (UBC), Vancouver, BC, Canada. His research interests include noncoherent detection, equalization, multiuser detection, MIMO systems, space–time processing, and coding.

Dr. Schober was a corecipient of the Best Paper Award of the German Information Technology Society (ITG) in 2001. In 2002, he received the Heinz Maier–Leibnitz Award of the German Science Foundation (DFG). He also received the 2004 Innovations Award of the Vodafone Foundation for Research in Mobile Communications. Since April 2003, he has been an Editor for Detection, Equalization, and MIMO for the IEEE TRANSACTIONS ON COMMUNICATIONS.



Mani Jain received the B.S. degree in electrical engineering from the National Institute of Technology, Kurukshetra, India, in 1995 and the M.A.Sc. degree in electrical and computer engineering from the University of British Colombia, Vancouver, BC, Canada, in 2004. Her M.S. thesis work was on the design of low-complexity and power-efficient receivers for Bluetooth systems.

From 1995 to 1999, she worked with Siemens PCNL, India, on the planning of digital telephone exchanges. Later, she worked for over a year with

Infosys Technologies, India, where she led a team of engineers for Cisco systems' optical switches testing project. Currently, she is working as a Design Engineer with Eion Inc, Ottawa, ON, Canada. Her association with the telecom industry has provided her a broad range of experience in technologies varying from PSTN switches, optical networks to wireless systems.